Extended Abstracts of the 2007 International Conference on Solid State Devices and Materials, Tsukuba, 2007, pp. 746-747

C-5-3 (Invited)

Giant TMR in CoFeB/MgO/CoFeB Magnetic Tunnel Junctions

Shoji Ikeda[1], Jun Hayakawa[2,1], Young Min Lee[1,3], Katsuya Miura[2,1], Ryutaro Sasaki[1], Fumihiro Matsukura[1], Toshiyasu Meguro[1] and Hideo Ohno[1]

[1] Laboratory for Nanoelectronics and Spintronics, RIEC, Tohoku Univ.,
2-1-1 Katahira, Aoba-ku, Senda 980-8577, Japan
Phone: +81-22-217-5555 E-mail: sikeda@riec.tohoku.ac.jp
[2]Advanced Research Laboratory, Hitachi, Ltd.,
1-280 Higashi-koigakubo, Kokubunji-shi, Tokyo 185-8601, Japan
[3] Present affiliation: Fujitsu Laboratories Ltd.

1. Introduction

Magnetic tunnel junctions (MTJs) with highly oriented (001) MgO barrier/ ferromagnetic electrodes, which offer giant tunnel magnetoresistance (TMR) ratio [1]-[7] at room temperature (RT) and current-induced magnetization switching (CIMS) at relatively low critical current density [8]-[11], have attracted much interest because of the application to spintronics devices such as spin transfer torque random access memory (SPRAM) and MTJ-based logic circuits[12]-[14]. Realizing high TMR ratios in sputtered CoFeB/MgO/CoFeB MTJs is of prime importance from a technology point of view, because sputtering is the preferred and established method for industrial applications. In this MTJ system, the TMR ratio of 500% at RT and 1010% at 5 K was recently observed [15]. However, the details of the CoFeB electrode composition and thickness which yield large TMR ratio for exchange biased (EB)-SV MTJs with MnIr pinning layer and pseudo-spin valve (P-SV) MTJs without MnIr have not yet been fully clarified.

In this work, we investigated the dependence of TMR ratio on CoFeB electrode composition and thickness for EB-SV and P-SV MTJs.

2. Experimental conditions

The rf-sputtered MTJs studied here have stacking structure of substrate/Ta(5)/Ru(20)/Ta(5)/NiFe(5)/ MnIr(8)/ CoFe (2.5) / Ru (0.8) / $(Co_xFe_{100-x})_{80}B_{20}$ (3) / MgO (1.5)/ $(Co_xFe_{100-x})_{80}B_{20}$(0-10)/Ta(5)/Ru(10) for EB-SV MTJs and Ta(5)/ Ru(20) /Ta (5) / $(Co_xFe_{100-x})_{80}B_{20}$ (2-7) /MgO (1.5, 2.1) / $(Co_xFe_{100-x})_{80}B_{20}$(4)/Ta(5)/Ru(10) for P-SV MTJs (in nm). In CoFeB layer, the B composition was fixed to 20 at% and the Co composition x was changed from 25 to 75 at%. The CoFeB layer thickness t_{CoFeB} was varied from 0 to 10 nm by using the slide shadow mask technique. All MTJs were fabricated by photolithography (electron-beam lithography) and Ar ion milling with a junction size of 0.8 × 4 (0.1 × 0.2) μm^2, and then were annealed at T_a = 270-525°C for 1h in a vacuum under 4 kOe. The TMR ratio was measured using a dc four probe method in the magnetic field range of ±3 kOe. Crystal structures were investigated by high resolution transmission electron microscopy (HRTEM) on samples prepared separately for its study; the stacking of the samples for HRTEM were substrate/Ta(5) /$(Co_xFe_{100-x})_{80}B_{20}$(3) /MgO(1.5)/ $(Co_xFe_{100-x})_{80}B_{20}$ (10)/Ta(3) with x = 25% and 75%.

3. Results and discussion

Fig. 1 shows TMR ratios measured at RT as a function of annealing temperature (T_a) for EB-SV MTJs with x = 50% and P-SV MTJs with x = 25% and 50%. The TMR ratios in these different MTJ types are approximately the same at T_a below 400 °C. The TMR ratio for P-SV continues to increase up to T_a =475 °C. In contrast, the TMR ratios for EB-SV start to decrease at T_a = 425 °C and continue decreasing. The TMR ratio of EB-SV with x = 50 annealed at T_a = 400°C reaches 361% at RT (578% at 5K). The P-SV MTJs with x = 50% annealed at 450-475 °C show the TMR ratio of 450% at RT (747% at 5K.) By replacing the $Co_{40}Fe_{40}B_{20}$ electrode with Fe-rich $Co_{20}Fe_{60}B_{20}$ in P-SV MTJs, the TMR ratio increased further to 472% at RT (804% at 5K). Energy dispersive x-ray analysis (not shown) reveals that annealing at 450°C induces interdiffusion of Mn and Ru atoms into the MgO barrier and ferromagnetic layers in EB-SV MTJs [7]. The interdiffusion of Mn and/or Ru is seemed to be one factor of the decrease in the TMR ratio at T_a= 425°C in EB-SV.

When the MgO thickness was increased from 1.5 to 2.1 nm, while maintaining the same electrode conditions (x = 25% and thickness 4.3 nm) as the P-SV MTJ that obtained the highest TMR ratio, a TMR ratio of 500% at RT was recorded. The TMR ratio at 5 K was 1010%.

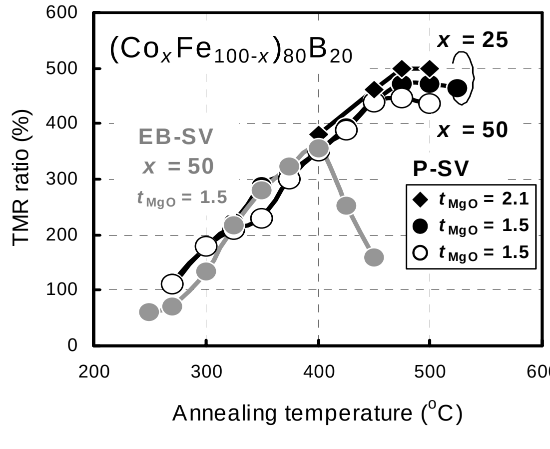

Fig.1. TMR ratio as a function of annealing temperature for EB-SV and P-SV MTJs having $(Co_xFe_{100-x})_{80}B_{20}$ electrode with x = 25 and 50.

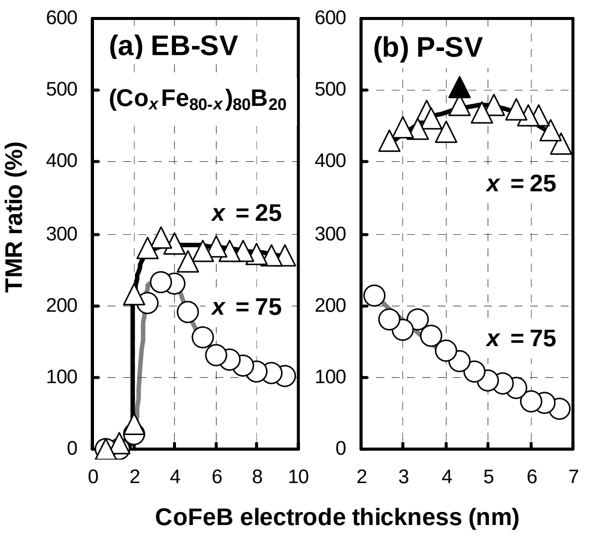

Fig.2. TMR ratio as a function of CoFeB electrode thickness for (a) EB-SV and (b) P-SV MTJs having $(Co_xFe_{100-x})_{80}B_{20}$ electrode with x = 25 and 75. Open symbols and a filled triangle correspond to MTJs with 1.5 and 2 nm- thick MgO barrier, respectively.

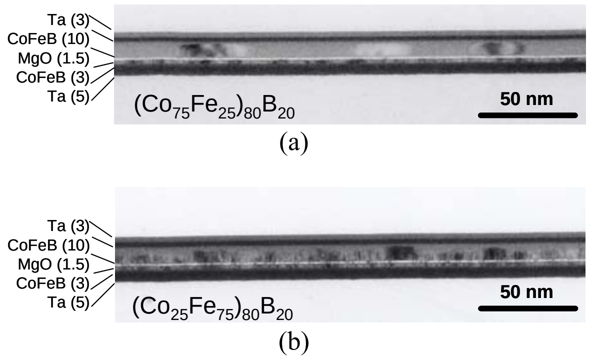

Fig. 3 Cross-sectional HRTEM images for Ta(5) / $(Co_xFe_{100-x})_{80}$ B_{20}(3) /MgO(1.5) /$(Co_xFe_{100-x})B_{20}$(10) /Ta(3) films with x = (a) 75% and (b) 25% annealed at 450 °C for 1 h.

Fig. 2 shows the TMR ratio as a function of the CoFeB electrode thickness (t_{CoFeB}) for EB-SV and P-SV MTJs with Co composition x = 25% and 75%, which are annealed at T_a= 375 and 475 °C, respectively. There is a clear difference among MTJs having different Co composition. For EB-SV MTJs with x=25% seen in Fig. 2(a), the TMR ratio is almost constant when t_{CoFeB} is more than 2nm. The EB-SV MTJs with x=75% showed a marked decrease of the TMR ratio with increasing t_{CoFeB}. As shown in Fig. 2(b), similar CoFeB thickness dependence was observed also in the P-SV MTJs.

To understand the CoFeB thickness dependence of the TMR ratio of the EB-SV and P-SV MTJs having different Co compositions, HRTEM was employed for structural characterization. Fig. 3 shows the cross-sectional HRTEM images of Ta(5) /$(Co_xFe_{100-x})_{80}B_{20}$(3) /MgO(1.5) /$(Co_xFe_{100-x})B_{20}$(10) /Ta(3) films with x = (a) 75% and (b) 25%, which were annealed at 450 °C for 1 h. As shown in Figs. 3(a) and (b), the 3-nm-thick bottom CoFeB electrodes in both samples crystallized into a bcc (001) texture, whereas the 10 nm-thick top electrodes developed different structural features depending on the Co composition. The top CoFeB electrode with x = 75% shown in Fig. 3(a) crystallized in a granular bcc (001) structure embedded in an amorphous matrix. In contrast, the top electrode with x = 25% shown in Fig. 3(b) crystallized to bcc (001) in the entire interface region adjacent to the MgO barrier. The low TMR ratio in the x = 75% sample with relatively thick CoFeB electrode can thus be explained as a result of inhomogeneous crystallization shown in Fig. 3(a).

4. Conclusions

The optimum annealing temperature (T_a=450-500°C) that results in the maximum TMR ratio for P-SV MTJs is higher than that (T_a = 400 °C) of EB-SV MTJs. The absence of diffusion of Mn and/or Ru into the MgO barrier at high T_a above 450°C is a factor for the high TMR ratios in P-SV MTJs. A remarkable difference in the CoFeB thickness dependence of TMR ratio between x = 25 and x = 75 is observed for the EB-SV and P-SV MTJs. From the cross-sectional HRTEM images, the difference in the crystallized structure of CoFeB electrode with x = 25 and x = 75 was observed, which appears to be one of the factors determining the difference of the film thickness dependence of the TMR ratio on the CoFeB composition. The maximum TMR ratio of 500% at RT (1010% at 5 K) was observed in a P-SV MTJ with 4- and 4.3-nm-thick $(Co_{25}Fe_{75})_{80}B_{20}$ electrodes, and 2.1-nm-thick MgO annealed at 475 °C.

Acknowledgements

This work was supported by the IT program of Research Revolution 2002 (RR2002): “Development of Universal Low-power Spin Memory” from the Ministry of Education, Culture, Sports, Science and Technology of Japan. The authors thank Iori Morita for support in this work.

References

[1] S. S. P. Parkin *ea al.*, Nat. Mater. **3** (2004) 862.
[2] S. Yuasa *et al.*, Nat. Mater. **3** (2004) 868.
[3] D. D. Djayaprawira *et al.*, Appl. Phys. Lett. **86** (2005) 092502.
[4] J. Hayakawa *et al.*, Jpn. J. Appl. Phys. **44** (2005) L1267;
[5] S. Ikeda *et al*., Jpn. J. Appl. Phys. **44** (2005) L1442.
[6] Y. M. Lee *et al.*, Appl. Phys. Lett. **89** (2006) 042506.
[7] J. Hayakawa *et al*., Appl. Phys. Lett. **89** (2006) 232510.
[8] H. Kubota *et al.*, Jpn. J. Appl. Phys. **44** (2005) L1237.
[9] J. Hayakawa *et al.*, Jpn. J. Appl. Phys. **44** (2005) L1267.
[10] Z. Diao *et al*., Appl. Phys. Lett. **87** (2005) 232502.
[11] J. Hayakawa *et al*., Jpn. J. Appl. Phy. **45** (2006) L1057.
[12] M. Hosomi *et al*., *IEDM Tech. Dig.* (2005) 459.
[13] T. Kawahara *et al.*, in *Proc. IEEE Int. Solid-State Circuits Conf. Dig. Tech. Papers* (2007) 480.
[14] S. Ikeda et al., IEEE Trans. Electron Devices **54** (2007) 991.
[15] Y. M. Lee *et al.*, Appl. Phys. Lett. **90** (2007) 212507.